J Low Temp Phys (2012) 167:102–107
DOI 10.1007/s10909-011-0431-4

A Two-Fluid Model for the Transition Shape in Transition-Edge Sensors

D.A. Bennett · D.S. Swetz · R.D. Horansky · D.R. Schmidt · J.N. Ullom

Received: 27 July 2011 / Accepted: 14 November 2011 / Published online: 24 November 2011

Abstract Superconducting microcalorimeters based on transition-edge sensors (TESs) are being successfully used in applications ranging from optical photon counting to gamma-ray and alpha particle spectroscopy. Practical instruments often require a complex optimization among speed, linearity and energy resolution. However, a lack of understanding of the superconducting transition limits our ability to predict the behavior of a new TES design. Specifically, there is an unmet need for a model that predicts the current and temperature dependent resistance surface that describes the transition: $R(I,T)$. This paper describes the predictions of a two-fluid model for the resistance of a TES based on a Ginzburg-Landau form of the critical current. We compare the predictions of the model for the logarithmic derivatives of resistance with temperature and current (α and β) to measurements of TESs used in x-ray and gamma spectrometers. The model shows excellent qualitative agreement that provides useful insight into the dependence of α and β on the current density and bias point of the TES.

Keywords Transition-edge sensors · Superconducting transition

1 Introduction

Transition-edge sensors (TES) have been successfully implemented in a number of applications despite our lack of understanding of the fundamental shape of the superconducting transition as a function of temperature and current [1]. The inability to predict the resistance of a TES under different operating conditions and with changing device parameters limits our ability to further optimize TES based instruments.

D.A. Bennett (✉) · D.S. Swetz · R.D. Horansky · D.R. Schmidt · J.N. Ullom
Quantum Devices Group, National Institute of Standards and Technology, Boulder, CO 80302, USA
e-mail: douglas.bennett@nist.gov

Furthermore, it is difficult to predict the behavior of TESs outside a small-signal approximation without an understanding of how the resistance changes with operating conditions.

An empirical form for $R(I,T)$ was proposed by Cabrera [2]. Also, predictions based on a Ginzburg-Landau theory for the relationship between the logarithmic partial derivative of resistance with respect to temperature, α, and current, β, have been proposed [3] and compared with data [4, 5]. Although these models predict some features of the data, they do not predict the general dependence of β on the bias point, $R(I,T)/R_n$, in the transition or as a function of the current at a constant bias point. In this manuscript, we compare the results of a two-fluid model of the resistance surface to measured values and demonstrate that it reproduces the general trends observed in the data.

2 Two-Fluid Model for the Resistance of a TES

Irwin et al. proposed using a simple two-fluid model to describe the total current through a TES biased in the resistive transition [6]

$$I(T) = c_I I_c(T) + \frac{V}{c_R R_n}, \tag{1}$$

where V is the voltage across the TES, I_c is the temperature dependent critical current and R_n is the normal resistance of the device. The model separates the super current, which is some fraction (c_I) of the critical current, and a quasiparticle current, which is equal to V divided by some fraction (c_R) of the normal resistance. This model is equivalent to the Skocpol-Beasley-Tinkham (SBT) model [7] of a resistive transition for a superconductor with phase slip lines (PSL) assuming a constant ratio of the time-averaged critical current to the critical current, $\overline{I_c}/I_c$. In the SBT model, $c_I = \overline{I_c}/I_c$ and $c_R = 2N\rho_\lambda \Lambda_{Q^*}/R_n$, where ρ_λ is the normal resistance per unit length, Λ_{Q^*} is the charge imbalance relaxation length, and N is the number of phase-slip lines. In this manuscript, we will start with the simplified form suggested by Irwin et al., in which we ignore the weak temperature dependence of Λ_{Q^*} and assume c_I and c_R are constants. In a more detailed model the constants would be a function of temperature and current and would include a mechanism for adding increasing numbers of phase-slip lines with increasing current.

With the assumption that c_I and c_R are constant, all the temperature dependence comes from I_c. In this regime a logical choice for $I_c(T)$ is the Ginzburg-Landau (GL) form for the critical current that describes I_c near the critical temperature, T_c. The GL critical current is given by

$$I_c(T) = I_{c0}\left(1 - \frac{T}{T_c}\right)^{3/2}, \tag{2}$$

where I_{c0} is the zero temperature critical current of the film.

We can use (1) to write the resistance of the film in a more suggestive form:

$$R(V,T) = \left(\frac{c_I I_c(T)}{V} + \frac{1}{c_R R_n}\right)^{-1}, \tag{3}$$

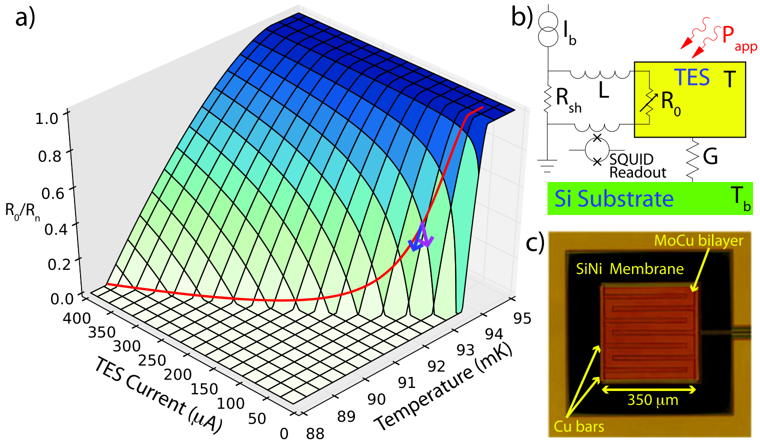

Fig. 1 (Color online) (**a**) Resistance surface in units of R_n as a function of T and I calculated by use of (3) for $c_I = 0.5$ and $c_R = 1$ and TES parameters for our typical x-ray device. The *solid red line* shows the (IV) trajectory for a TES, (4). (**b**) A schematic representation of a TES and (**c**) a photograph of the x-ray TES that was used to test the model

which is just the sum of two parallel resistance paths. Equation (3) can also be viewed as the resistance of two noninteracting fluids: a super-current fluid and a normal fluid. Figure 1a shows the model's prediction for the $R(I, T)$ surface in units of R_n for $c_I = 0.5$ and $c_R = 1$ and parameters for the TES described in detail in the next section. Unlike the $R(I, T)$ surface proposed by Cabrera [2], increasing the current both shifts and widens the transition.

To compute the trajectory of current versus voltage (IV) on this surface, we need additional information about the thermal power flowing from the TES into the heat bath. The steady-state TES temperature (T_0) is determined by the power balance between the Joule heating of the bias, the incident power to be measured (P_{app}) and the power flowing though the TES thermal conductance, given by

$$\frac{V^2}{R(V, T)} + P_{app} = k(T^n - T_b^n), \tag{4}$$

where k is the thermal conductivity, n is the thermal conductance exponent and T_b is the bath temperature. At a given voltage bias, this equation can be solved for T to find T_0, which then determines the steady-state resistance R_0 and current I_0. The red solid line in Fig. 1a shows the trajectory of this solution superimposed on the resistance surface for $P_{app} = 0$, $k = 11.7\ \text{nW}/K^n$, $n = 2.45$, and $T_b = 70$ mK.

When a photon strikes a microcalorimeter, the instantaneous current and temperature are described by a set of coupled differential equations that describe the TES in the small-signal limit [1, 8]. I_0, T_0 and R_0 are the initial conditions for these equations. When modeling the response of the TES, only the linear terms are kept in the expansion of the resistance, so that changes in current in the small-signal limit are described by the logarithmic derivatives of the resistance with respect to temperature at constant current, $\alpha_I = (T_0/R_0)(\delta R/\delta T)|_{I_0}$ and with respect to current at constant temperature, $\beta_I = (I_0/R_0)(\delta R/\delta I)|_{T_0}$. These derivatives are shown in Fig. 1a for a bias point near 50% R_n by a blue (α_I) and a purple (β_I) arrow. Understanding TES behavior in the large-signal limit is reduced to understanding how α_I and β_I vary over the resistance surface.

Using (3), we can solve for α_I and β_I at any point on the surface. At constant current, $(\delta R/\delta T)|_{I_0} = (1/I_0)(\delta V/\delta T)$, so that

$$\alpha_I = \frac{T_0}{R_0 I_0}\frac{\delta V}{\delta T}. \tag{5}$$

We can then take the partial derivative of (3) with respect to V, assuming c_I and c_R are constant, and substitute into the expression for α_I to get

$$\alpha_I = \frac{3}{2} c_I c_R \frac{R_n}{R_0}\frac{I_{c0}}{I_0}\frac{T_0}{T_c}\left(1 - \frac{T_0}{T_c}\right)^{1/2}. \tag{6}$$

For β_I we can rearrange the derivatives of resistance at constant temperature as $(\delta V/\delta I) = R_0 + I_0(\delta R/\delta I)$, which when written in terms of β_I gives

$$\beta_I = \frac{1}{R_0}\frac{\delta V}{\delta I} - 1. \tag{7}$$

At constant c_R, we arrive at a very simple form for β_I:

$$\beta_I = c_R \frac{R_n}{R_0} - 1, \tag{8}$$

which depends only on c_R and the bias point. Specifically, at a given bias point, β_I does not depend on the current.

3 Comparison with Data

This simple model of the transition takes no consideration of the geometry of actual devices, such as the superconducting leads or normal metal bars [1], and can not possibly predict subtle differences in the transition that are observed for small changes in the geometry. However, it is interesting to explore whether this model can describe some of the general trends that are observed in TESs. In this section, we compare the predictions for the IVs, α_I and β_I to measurements of one of our standard TESs used for x-ray microcalorimeters.

Figure 1b shows a schematic of our voltage biased TES and the SQUID amplifier used to measure the TES current. The device measured in this comparison, shown in Fig. 1c, is a MoCu bilayer TES that is 350 μm by 350 μm on a silicon nitride membrane with seven copper bars. Various characterization measurements were performed to determine the parameters relevant to the model. $R_{sh} = 0.3$ mΩ was measured from its Johnson noise as a function of temperature and verified by four-point resistance measurements of other chips from the same wafer. $R_n = 9.0$ mΩ and a parasitic resistance of less than 1 μΩ are then extracted from the normal and superconducting parts of the IV curves. $T_c = 94.1$ mK and $G(T = T_c) = 124$ pW/K were extracted from power-law fits to measured IVs at different T_b. Fitting the power at a constant % R_n to extract G assumes $\beta_I = 0$ and should be performed at biases near

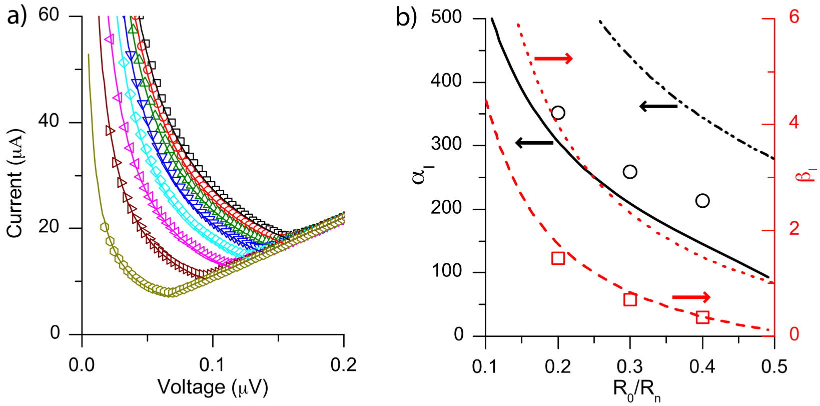

Fig. 2 (Color online) (**a**) IVs for the device shown in Fig. 1b measured at successive bath temperatures; 55 mK (*black squares*) to 90 mK (*yellow hexagons*) in steps of 5 mK. The lines are the predictions of the model at each temperature by use of the measured device parameters and $c_R = 1$, $c_I = 0.5$ and $I_{c0} = 55$ mA. (**b**) The measured α_I (*black circles*, *left axis*) and β_I (*red squares*, *right axis*) at 20%, 30%, and 40% R_n along with the calculations from the model for the same parameters except at two different values of c_R, $c_R = 1$ (α_I *black dash dot line*, β_I *red dotted line*) and $c_R = 0.55$ (α_I *black solid line*, β_I *red dashed line*)

the top of the transition where β_I is small, and extrapolated via the temperature dependence to values lower in the transition. The measured β_I were extracted from fits to complex impedance data at high frequencies, and the values of α_I were extracted from fits to thermal pulses created by photons incident from a diode laser. The heat capacity (C) was extracted from fits to pulses at a bath temperature close to T_c and a bias point around 99% R_n where the electrothermal feedback is small and the decay time of the pulse is dominated by G and C.

Figure 2 shows the measured IV at eight different temperatures from 55 mK to 90 mK. Each temperature has a corresponding fit to the numerical solution of (4) with the model parameters $c_R = 1$, $c_I = 0.5$ and $I_{c0} = 55$ mA. The model agrees well with the data over the whole temperature range. This agreement does not necessarily imply a good fit to α_I and β_I individually, because the IV curves move on a trajectory that is a combination of both of these parameters. Figure 2b shows the measured α_I (black circles, left axis) and β_I (red squares, right axis) at three different bias points; 20%, 30% and 40% R_n. The lines are predictions of the model for α_I using (6), $c_R = 1$ (black dash dotted line) and $c_R = 0.55$ (black solid line), and β_I using (8), $c_R = 1$ (red dotted line) and $c_R = 0.55$ (red dashed line). At $c_R = 1$, the model over-predicts β_I by almost a factor of two. However, at $c_R = 0.55$, the model is consistent with the measured values, and the general trend is consistent with similar data from other groups [4, 5].

Figure 3 shows the measured α_I and β_I for the same device, but as a function of the current at two constant bias points, 20% R_n (blue circles) and 30% R_n (green triangles). The current was varied while keeping the bias point constant by changing T_b. Equations (6) and (8) are plotted at 20% R_n (blue solid line) and 30% R_n (green dashed line) for $c_R = 0.55$. The model reproduces the general trend of the data, except for the bumps in the data at 25 μA for 20% R_n and 14 μA for 30% R_n.

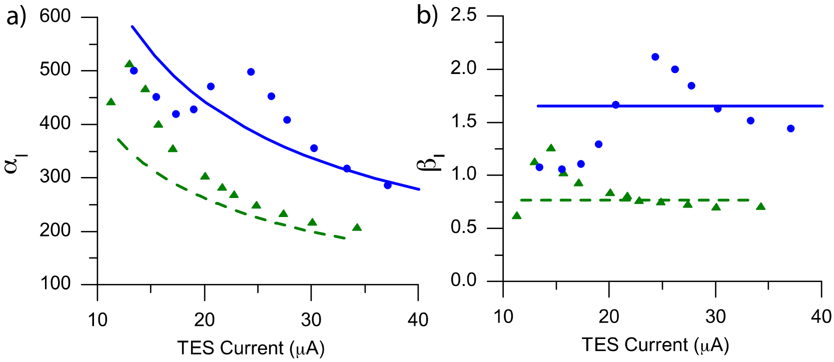

Fig. 3 (Color online) The measured and calculated values of (**a**) α_I and (**b**) β_I as a function of TES current for one of our standard x-ray devices. The data measured at 20% R_n are shown as *blue circles*, while the data at 30% R_n are as *green triangles*. The *blue solid lines* and the *green dashed lines* are the predictions of the model at $c_R = 0.55$ and $c_I = 0.5$

This fine structure is likely due to physics not included in this simple version of the model using constant values of c_R and c_I. In general, β_I shows no general trend with current, and α_I is roughly inversely proportional to I_{c0}/I_c.

4 Conclusions

An accurate model of the superconducting transition in TESs is important in understanding devices operating in the large-signal limit and will be a useful tool for TES design and characterization. In an effort to evaluate one possible model, we have calculated α_I and β_I for a simple two-fluid model of the transition in order to compare the predictions with measurements of practical devices. The model accurately predicts the shape of IV curves along with the general dependencies of α_I and β_I with changes in current and temperature. Future work will focus on techniques for predicting the parameters c_R and c_I, as well as on understanding the detailed effects of different device geometries.

Acknowledgements We gratefully acknowledge the support of the US Department of Energy through the Office of Nonproliferation Research and Development.

References

1. K.D. Irwin, G.C. Hilton, Transition-edge sensor, in *Cryogenic Particle Detection*. Topics in Applied Physics, vol. 99 (Springer, Berlin, 2008)
2. B. Cabrera, J. Low Temp. Phys. **151**, 82 (2008)
3. Y. Takei, R. Fujimotoa, Y. Ishisaki et al., Nucl. Instrum. Methods A **520**, 340 (2004)
4. S.J. Smith, S.R. Bandler, A.D. Brown et al., J. Low Temp. Phys. **151**, 195 (2008)
5. M.A. Lindeman, K.A. Barger, D.E. Bradl et al., J. Low Temp. Phys. **151**, 190 (2008)
6. K.D. Irwin, G.C. Hilton, D.A. Wollman, J.M. Martinis, J. Appl. Phys. **83**, 3978 (1998)
7. W.J. Skocpol, M.R. Beasley, M. Tinkham, J. Low Temp. Phys. **16**, 145 (1974)
8. M.A. Lindeman, S. Bandler, R.P. Brekosky et al., Rev. Sci. Instrum. **75**, 1283 (2004)